

A Novel Fracture Mechanics Approach to Determine the Threshold Stress Intensity Factor in Corrosive Environment

Sarvesh Pal¹, R.K. Singh Raman^{1,2}, R.N. Ibrahim¹

¹ *Department of Mechanical and Aerospace Engineering*

² *Department of Chemical Engineering*
Monash University, Vic 3800, Australia

ABSTRACT

This paper investigates the method to determine the K_{ISCC} of grade 250 steel and simulated heat affected zone (SHAZ) in 30% caustic solution at 100°C using CNT technique. Stress corrosion cracking has been confirmed using scanning electron microscope. Crack growth rate in caustic solution has been determined by CNT technique.

1 INTRODUCTION

The essential components of stress corrosion cracking are a metal susceptible to a potent environment and a state of stress that exceeds some threshold value. Stress corrosion cracking is considered to be the most dangerous form of failure since corrosion crack may propagate undetected to leak or sudden failure. Undetected stress corrosion cracking of in-service components has long been responsible for major safety concerns, waste in production time and cost in the maintenance of the materials in some of major Australian industries, such as chloride SCC in marine applications, caustic SCC in alumina processing, pulp and paper industries.

Despite the scale of this problem, there have been very limited studies on the development of a cost-effective technique for monitoring of SCC by a fracture mechanics approach. The fracture mechanics approach for studying the susceptibility of engineering materials to SCC provides essential data for the design and prediction of life, which the non-fracture mechanics method are unable to do.

Industrial experience highlights the need for a fresh approach to investigate the failed components and development of a simple monitoring technique. Accurate monitoring of SCC crack growth and life prediction can be carried out by the fracture mechanics approach. However, the traditional standard fracture mechanics techniques (centre cracked (CC), surface flawed (SF), cantilever bend (CB), double cantilever beam (DCB), and compact tension (CT) specimens) [1] are prohibitively expensive, time-consuming, bulky and sometimes the required sample size is hard to procure (e.g. from a failed thin component which restricts the use of the commonly techniques for SCC monitoring).

There is a need for a technique which can overcome the disadvantages described above. A novel approach has been developed in recent years [2] for determination of the stress intensity factor (K_I) and threshold stress intensity factor for stress corrosion cracking (K_{Isc}) for propagation of stress corrosion cracks, using small diameter circumferential notched tensile (CNT) specimens [3]. This feature of CNT specimens will enable testing of thin section failed component as well as lower the cost of testing.

The application of the CNT specimens to the research problems in SCC will permit mechanical loading of the specimens in the corrosive environment, use of pre-cracked specimens with known K_I values at the crack tip and testing of a relatively large number of specimens due to reduced costs and lower material requirements for fabrication of specimens as well as the testing rigs.

The CNT specimen is the smallest possible specimen that can produce valid plane strain loading conditions within $\pm 3\%$ of the results determined using the ASTM standard compact tension (CT) test specimens [4, 5]. Acceptable results have been achieved [6] using 9.5 and 15 mm diameter CNT specimens whereas for the same material, fracture toughness (K_{Ic}) determination, using standard CT specimens, requires dimensions up to 80 mm.

In alumina industry, steel is commonly used material for construction of welded reaction vessels with different capacities as digesters, decomposer and precipitator. SCC is observed during service and many of these cracks are close to the welded zone. During welding metallurgical changes occur, which creates different microstructure with different mechanical and electrochemical properties. The microstructure of the weld and heat affected zone (HAZ) depends not only on the chemical composition of the parent metal but also profoundly on the welding thermal cycle. The HAZ in the vicinity of the fusion zone undergoes severe thermal cycle due to flow of intense local heat [7]. As a result the microstructure of HAZ changes. The final microstructure depends on the chemical composition of the steel, maximum temperature and cooling rate. The cooling rate depends on the energy input of the welding process, initial temperature and the thickness of the specimen. The width of HAZ of carbon/mild steel depends on the temperature gradient and carbon content of the parent metal. A variety of microstructure can be found in mild steel weldment varying from fine martensite to coarse pearlite. As the width of HAZ is very narrow, the determination of K_{Isc} of HAZ by conventional techniques is even more difficult. HAZ is a narrow area (a few mm wide), producing a notch in such a narrow area may be a difficult task. However when the HAZ is simulated over a wide area using a precise thermo mechanical simulator then it may be easier to ensure that the notch stays in the simulated HAZ during the testing.

2 EXPERIMENTAL PROCEDURES

2.1 Material

The test material used in this investigation was grade 250 mild steel plates. The chemical composition and mechanical properties of this steel are listed in Table I and Table II.

Table I - Chemical composition of Grade 250 steel (wt%)

C	Si	Mn	P	S	Cu	Cr	Ni	Mo	V	Al	N
0.17	0.27	1.19	0.19	0.09	0.02	0.02	0.01	0.02	0.03	0.28	0.03

Table II -Mechanical properties of Grade 250 steel

YS	UTS	Elongation
M Pa	M Pa	%
338	492	35

2.2 Simulation of HAZ

In order to study the behaviour of HAZ microstructure of manual metal arc welding in caustic solution, the microstructure was simulated on Gleeble simulator at University of Wollongong, NSW Australia. The CNT specimens were held in a pair of water cooled copper grips one of which is fixed and other movable. The gap between the jaws was fixed to 35 mm to have uniform heating and cooling in the area to be exposed to the caustic environment.

The temperature gradient has been observed across centre and top of the notch to find out difference in temperature at notch and top of the notch. Two thermocouples were connected to the notched specimen in such a way that one

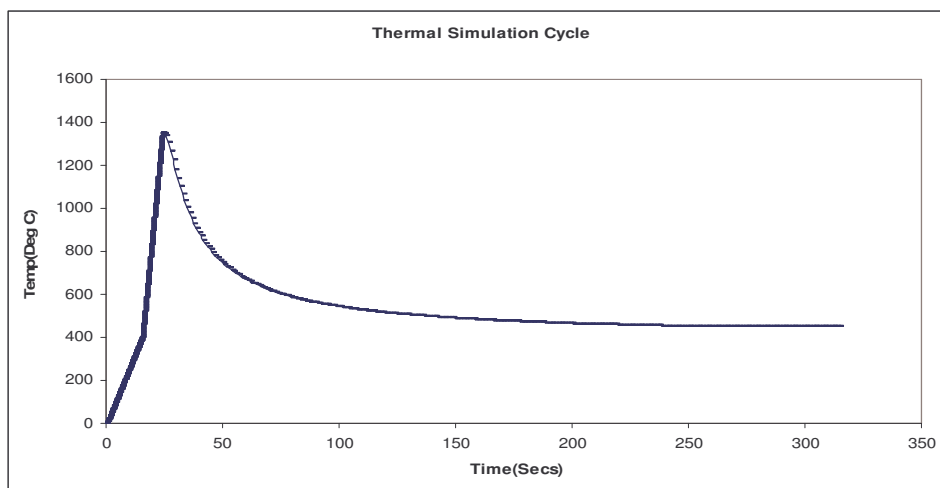


Figure 1 Thermal cycle for simulation HAZ

thermocouple wire was attached at centre of the notch, while other was fixed on the top the notch. The highest temperature for simulating weld thermal cycle was

1350°C. Normally this is the maximum temperature HAZ experience during manual arc welding process. The cooling time from 800°C to 500°C was controlled to 90 seconds to achieve a cooling rate 3.3°C/s to achieve the desired microstructure. The thermal cycle experienced by CNT specimen during simulation is shown in figure 1.

2.3 Circumferential notch tensile (CNT) technique for SCC testing

This relatively simple fracture mechanics based technique for SCC testing was recently developed at Monash University to determine the K_{ISCC} of engineering materials [8, 9]. CNT rig (Fig.2) is being used to generate K_{ISCC} data of HAZ. This technique simplifies and speeds up the testing procedure as well as provides considerable cost advantage over the conventional fracture mechanics techniques.

This rig has a corrosion cell made from Monel, which can sustain high pressure and temperature. The load is applied through Belleville springs. The corrosion cell is heated using band heater and temperature is controlled by digital temperature controller. Time counter is connected to CNT rig in such a way that when specimen fails, the counter stops and time to failure is determined. Safety arms are provided to stop ejection of specimen after failure.

The use of the CNT specimen [9] (Fig. 3) has many critical advantages. The small cross-section of the specimen makes it possible to load the specimen to quite high stress levels using moderate loads. Reducing material requirement is critical when the role of microstructure in the limited size such as weld and HAZ is to be investigated. The relevant microstructures need be produced only in the small volume of metal where notch can be easily produced. The CNT specimen is also less expensive to produce because of its cylindrical shape, which reduces the cost of specimen fabrication by a factor of up to 10 (c.f. CT specimen). In the cases where there is insufficient material available from a failed component to machine a long CNT specimen, short CNT specimens are machined at the available length then elongated by joining extension rods through welding or threading, since the region of interest is the notch region only. The connecting rods have been used to increase the length of simulated HAZ specimen in the present study.

CNT specimens were subjected to fatigue pre-cracking by a rotating bending machine. The surface of the fatigue pre-cracked specimen was polished with 400/800/1200/2000 grit paper. The pre-cracked specimens were washed with ethanol and dried before being installed into the SCC testing rig. A Teflon tape was wrapped around the CNT specimens to ensure that only the notch portion is exposed to the environment. The corrosion cell was filled with the caustic solution (300gpl, NaOH). The test rig was heated to the test temperature (100°C) before applying the tensile load to the specimen.

This procedure ensured that the applied load did not change as a result of the expansion of the specimen and surrounding fittings. The loading was carried out using INSTRON tensile testing machine. The specimens were held in the caustic solution at an applied load until they failed. The time-to-failure is recorded at instance of failure of the specimen. Tests were carried out at different values of applied K_I .

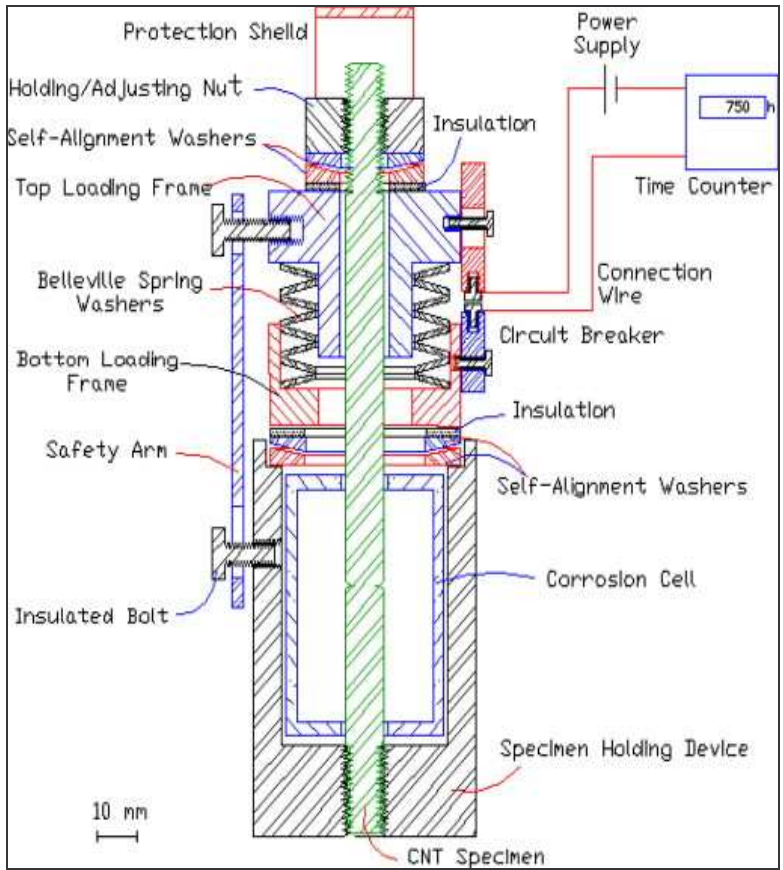


Figure 2 CNT rig for SCC testing

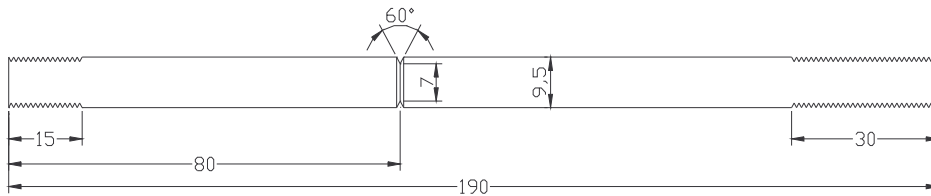


Figure 3 CNT specimen (all dimensions are in mm)

2.4 Determination of stress intensity factor (K_I)

The profile projector was used to measure the circular fatigue crack depth of the specimen. The top view of the specimen is divided into 12 wedge shaped elements with an interval of 30° for each wedge shaped element. Using profile projector, the radial depth of fatigue crack, a_f , and the machined groove depth, a_m , were measured. The detailed calculation can be found elsewhere [9].

2.4.1 Validity requirements for fracture toughness measurements of small cylindrical specimen

The formulations used to calculate the fracture toughness, K_{IC} of the material were based on linear elastic fracture mechanics (LEFM) which is valid if the specimen is deformed in an elastic manner. In practice, the specimen undergoes some plastic deformation before they fracture [4].

Validity requirements for plane strain fracture toughness evaluation are mentioned below:

- (1) The size of the deepest fatigue crack must be at least twice the size of the Irwin's correction factor.

$$a_f \geq 2 r_y \quad (1)$$

It was found that shallow cracks failed to provide the radial constraint required for the plane strain conditions. It was also found that shallow cracks resulted in a large plastic deformation zone. Therefore crack depth is an important validity requirement.

- (2) Stress applied on the specimen must not be greater than 2.5 times the tensile yield strength of the material.

$$\frac{\sigma_N}{\sigma_y} \leq 2.5 \quad (2)$$

where $\sigma_y = 0.2\%$ off set yield stress in Pascal.

2.5 Crack growth rate

Crack growth rate is determined by measuring the longest crack length and dividing it by the time of test. The crack growth rates are determined at different K_I values and plotted against K_I . In this paper, crack growth rate is being determined using the following formula:

$$\text{Crack growth rate } da/dt = dK_I/dt * da/dK_I \quad (3)$$

where a is the crack length (mm), t is time (hrs). The term dK_I/dt of equation is determined by the differentiating the relationship between K_I and time to failure (T_f). Second term da/dK_I is determined from relationship for deriving K_I from crack depth force [2, 10].

2.6 Fractography

The fracture surface was ultrasonically cleaned with a cleaning solution that contained 6 ml conc. HCl + 10 ml of 30 gpl 2 Butyne -1,4 diol + 100 ml distilled water. Cleaned surface was observed under JEOL 840 scanning electron microscope (SEM) in order to investigate the fractographic evidence of SCC of steel in caustic solutions i.e., inter- or trans-granular cracking.

3 RESULTS

3.1 Microstructure of simulated HAZ

The simulated HAZ specimens were sectioned and polished up to 3 μ level. The polished surface was etched with Nital etchant. The optical microstructure of simulated HAZ (SHAZ) at the centre of the notch contains needles of martensite (Fig. 4a and Fig. b), as the martensite is formed under the controlled cooling from 800°C to 500°C. However for cooling from 500°C to room temperature, the specimens were air cooled. This simulation process is dual in nature. In first instance the martensite is formed and then transformed to tempered martensite. The microstructure of base metal contains ferrite and pearlite (Fig. 4c).

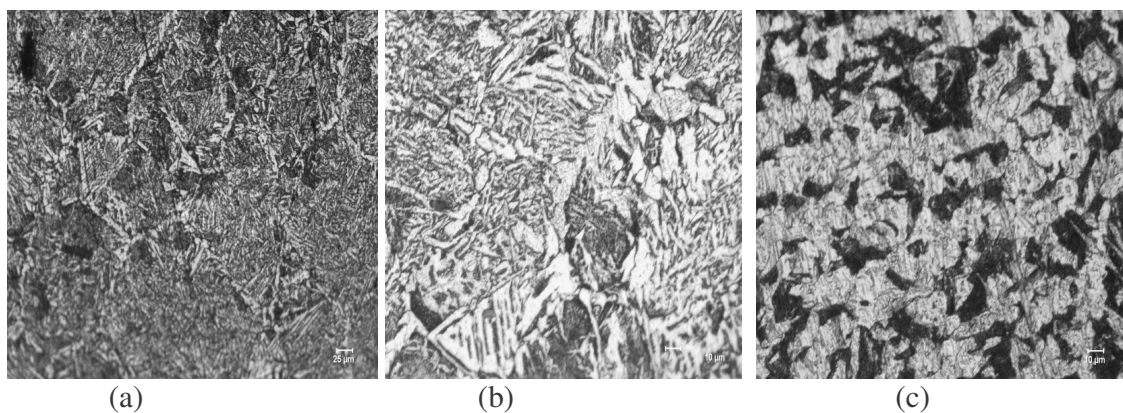


Figure 4 Microstructure of (a,b) simulated heat affected zone showing tempered martensite structure (c) parent metal showing ferrite and pearlite structure

3.2 K_{ISCC} of grade 250 steel in 30% caustic solution

The fracture surface of broken specimen was ultrasonically cleaned and observed under scanning electron microscope. The three different zones viz. fatigue crack zone, SCC zone and mechanical failure zone (Fig. 5a) were observed. At higher magnification, the SCC zone (Fig 5b) shows inter-granular features, which indicate that grade 250 steel at 100°C is susceptible to stress corrosion cracking in 30% caustic solution. Figure 5c shows the ductile features (dimples) in the centre part of the fracture surface which confirms that the failures to be purely mechanical. Beach mark shown in figure 5(d) shows the fatigue crack zone.

Fatigue pre-cracked CNT specimens of grade 250 steel were loaded in 30% caustic solution at different stress intensity levels. The specimens failed after different durations depending on the applied stress intensities. The stress intensity (K_I) against time of failure relationship for the base metal is shown in figure 6. The maximum time taken for a specimen to fail was 815 hrs i.e. at a K_I of 25.8 $\text{MPa m}^{1/2}$. However at 50 $\text{MPa m}^{1/2}$, it took only 40 h for the specimen to fail. As the stress corrosion crack propagates, the stress intensity increases until it reaches the critical value K_{IC} , which leads to purely mechanical failure (shown in Fig. 5c).

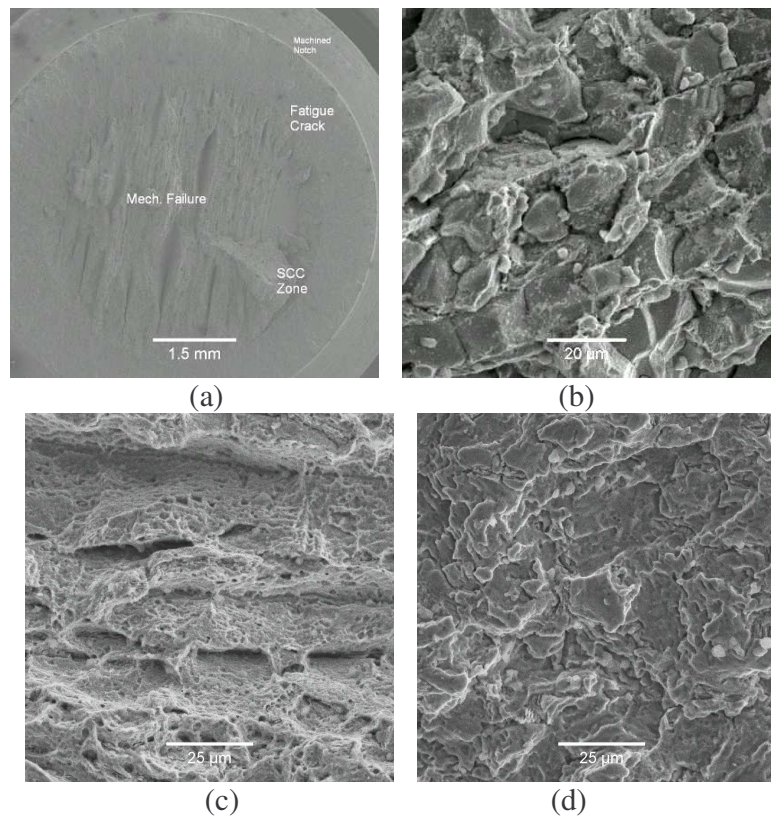


Figure 5 Scanning electron microscopic observations for grade 250 steel: (a) Overall fracture surface having machine notch, fatigue crack area, SCC zone and mechanical failure zone, (b) SCC Zone (c) Mechanical failure zone at a higher magnification.(d) Fatigue crack area

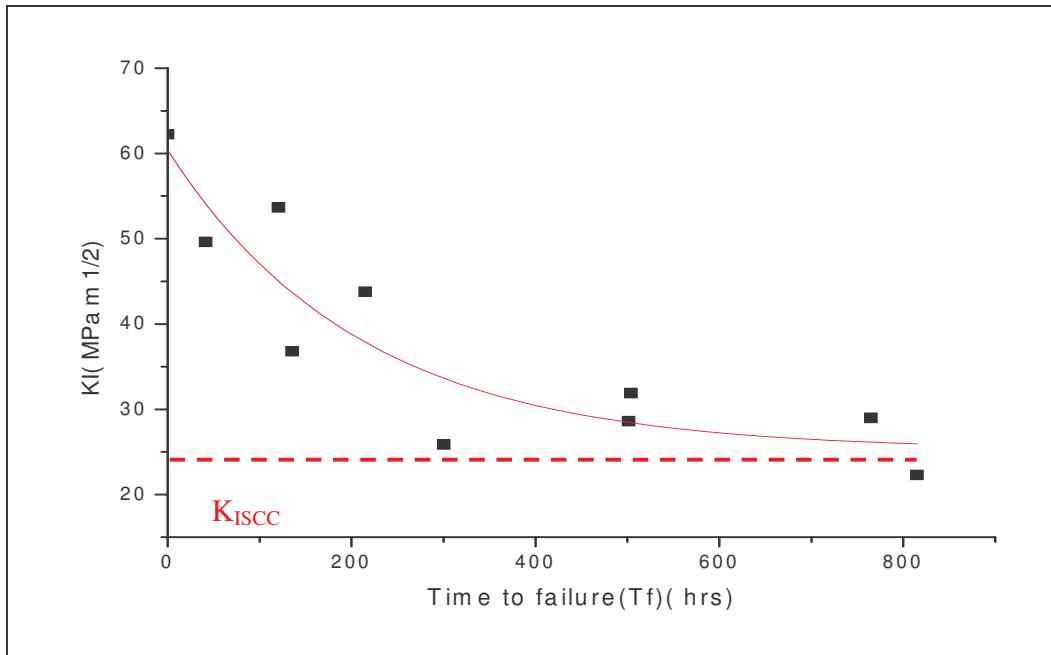


Figure 6 K_I vs. Time to failure graph for Grade 250 steel in 30% caustic solution at 100 °C

The relationship between stress intensity (K_I) and time to failure (T_f) is determined by the K_I vs. T_f graph in figure 6. The determined equation for the graph in figure 6 is

$$K_I = 25.23 + 35.16 * \exp(-T_f/210) \quad (4)$$

This equation is determined by the origin software. By putting $T_f = \text{infinity}$ the K_{ISCC} value is obtained. Therefore the K_{ISCC} of grade 250 steel is approx 25.23 $\text{MPa m}^{1/2}$ by equation 4, however the K_{ISCC} indicated in graph is 25 $\text{MPa m}^{1/2}$ which is close in approximation. By putting $T_f = 0$ the $K_I = 60.39 \text{ MPa m}^{1/2}$ is obtained. This is also in close approximation of the K_{IC} value determined experimentally.

3.3 K_{ISCC} of simulated HAZ of grade 250 steel

The overall fracture surface and different areas of simulated HAZ specimens (Fig.7) were similar to corresponding areas of base metal specimen. K_I vs. time to failure relationship for SHAZ is shown in figure.8. The Threshold value for SHAZ is approximately 47 $\text{MPa m}^{1/2}$.

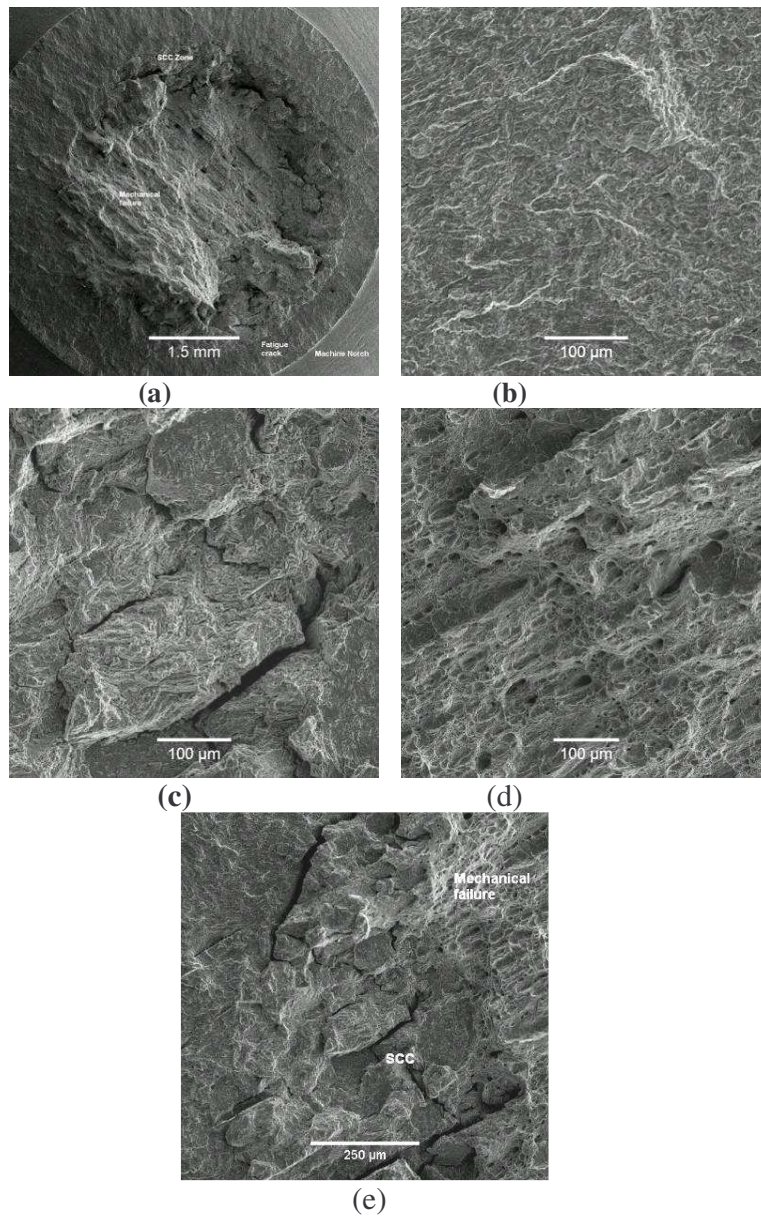


Figure 7 Scanning electron microscopic observations for simulated heat affected zone in Grade 250 steel: (a) Overall fracture surface having machine notch, fatigue crack area, SCC zone and mechanical failure zone, (b) Fatigue failure zone at higher magnification, (c) SCC zone, (d) Mechanical fracture zone and (e) SCC and mechanical fracture zone [11]

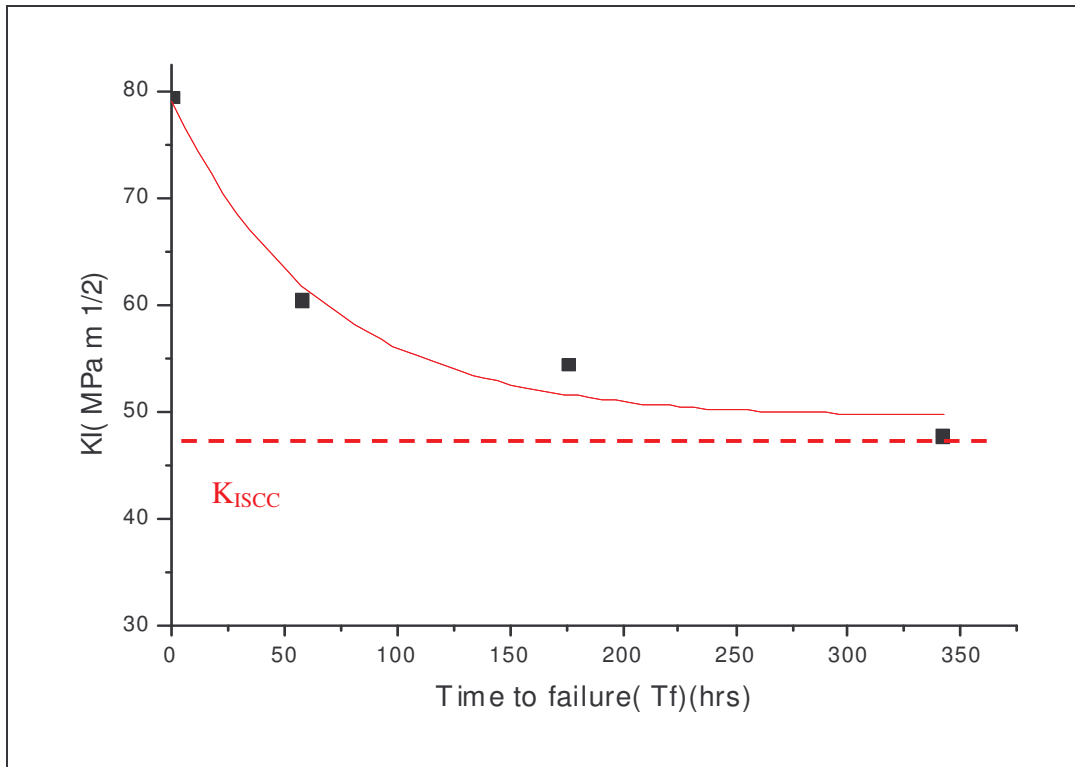


Figure 8 K_I vs. Time to failure graph for simulated HAZ of grade 250 steel in 30% caustic solution at 100 °C (More specimens were still running at the time of writing the article)

The relationship between stress intensity (K_I) and time to failure (T_f) is determined by the K_I vs. T_f relationship. The equation for the graph in figure 8 is given following

$$K_I = 49.46 + 29.63 * \exp(-T_f/66.52) \quad (5)$$

By putting $T_f = \text{infinity}$ in equation 5 K_{ISCC} value is obtained. Therefore the K_{ISCC} of simulated HAZ of grade 250 steel is approx 49.46 MPa m^{1/2} determined by equation, however the K_{ISCC} indicated in graph is 47 MPa m^{1/2} which is close in approximation. By putting $T_f = 0$ in equation 5 $K_I = 79.09$ MPa m^{1/2} is obtained. This value is also in close approximation of the K_{IC} value determined experimentally.

3.4 Crack Growth Rate and K_{ISCC} of base metal and simulated HAZ

The crack growth rate was calculated as discussed in section 2.5. Figure 9 and 10 represents the graphs for crack growth against K_I for parent metal and simulated HAZ respectively. In these graphs the crack growth rate increases with increasing stress intensities. The stress intensity, at which the crack growth is zero, implies that crack will not propagate. The intersection point gives threshold stress intensity factor for grade 250 steel at the above mentioned conditions (caustic environment and temperature of 100 °C). For crack to propagate the stress intensity should be more than K_{ISCC} . Figure 9 shows that the K_{ISCC} for base metal is approx 27 MPa

$m^{1/2}$, whereas figure 10 gives a threshold of approximately 49 MPa $m^{1/2}$ for simulated HAZ of grade 250 steel. This is in reasonably good approximation with the value determined by the K_I vs T_f relationship.

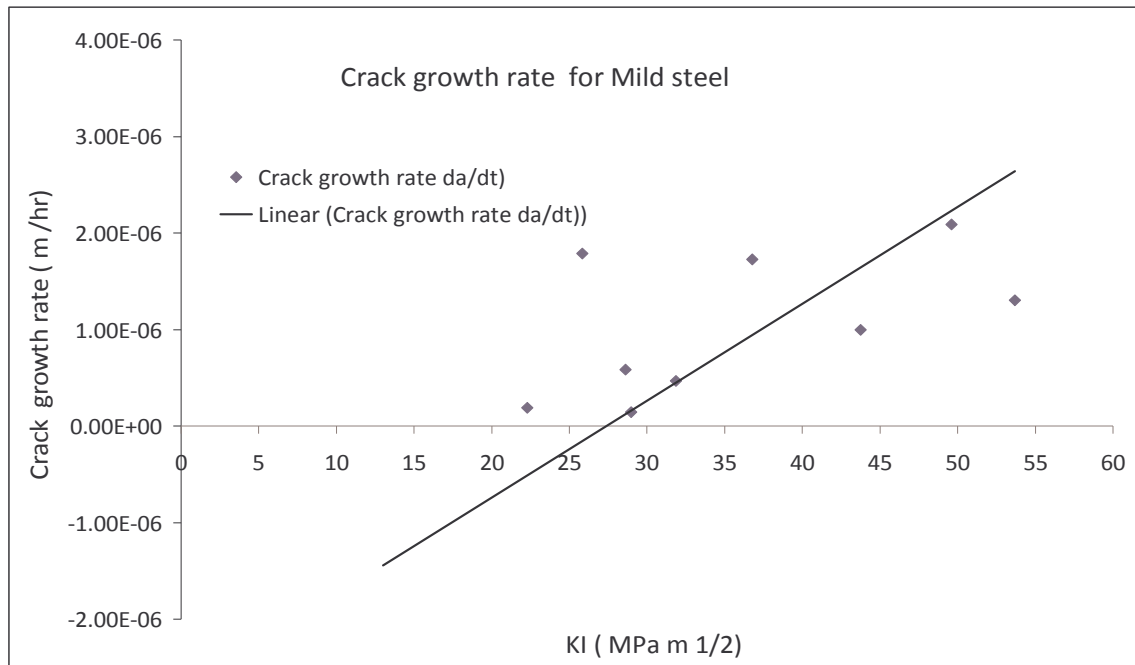


Figure 9 Crack growth of grade 250 steel in 30 % Na OH at 100 ° C

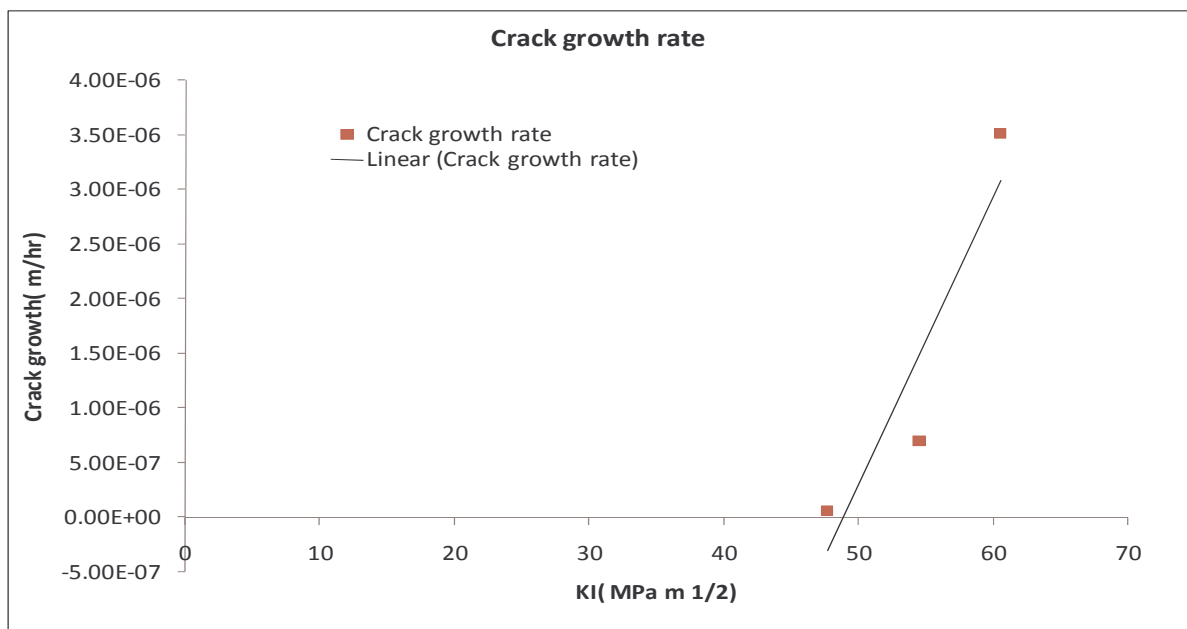


Figure 10 Crack growth of Simulated HAZ in 30 % Na OH at 100 ° C

4 DISCUSSION

It can be noticed that K_{ISCC} value for simulated HAZ is higher than the base metal. The higher K_{ISCC} value can be explained by the different microstructure of simulated HAZ compared with microstructure of parent metal. The parent metal contains ferrite and pearlite, whereas the SHAZ contains tempered martensite. Martensite is hard phase whereas ferrite and pearlite are comparatively softer. Arsenault and Ghali [12] suggested that crack follows the path of soft grain boundaries of ferrite than harder phase martensite and bainite. The microstructure of parent metal is more susceptible to SCC than the microstructure of the weld joint and the HAZ. Crack propagation rate in both cases, increases with increasing K_I . In case of parent metal and simulated HAZ the crack growth in caustic solution does not follow the well known three stage behaviour. However the crack growth rate increases monotonically. The continuous increasing crack growth rate against K_I of 4140 steel subjected to 33% NaOH has been reported in literature[13]. Fracture toughness of tempered martensite is higher than tempered bainite, ferrite and pearlite reported in literature[7, 14]. Therefore, there is a possibility of higher K_{ISCC} for tempered martensite than parent metal.

5 CONCLUSIONS

CNT testing approach was used to investigate the susceptibility of grade 250 steel to caustic corrosion cracking. These tests have provided K_{ISCC} data for parent metal and simulated HAZ at 100 ° C. The K_{ISCC} of parent metal and simulated HAZ are 25 MPa m^{1/2} and 47 MPa m^{1/2} respectively. Higher K_{ISCC} of simulated HAZ is due to microstructure present at the notch.

6 ACKNOWLEDGEMENTS

The authors would like to thank Australian Research Council Linkage Grant for financial support. A special word of appreciation to Prof Elena Pereloma, University of Wollongong for her kind support in using the simulation facility.

7 REFERENCES

1. Sedriks, A.J., *Stress corrosion cracking test methods*. Corrosion Testing Made Easy, ed. B.C. Syrett. Vol. 1. 1990.
2. Stark, H.L. and R.N. Ibrahim, *Crack propagation at constant load and room temperature in an extruded aluminium*. Engineering Fracture Mechanics, 1988. **30**(3): p. 409-414.
3. R.N. Ibrahim and H.L. Stark, *Establishing K_{IC} from eccentrically fatigue cracked small circumferentially grooved cylindrical specimens*. International Journal of Fracture, 1990. **44**: p. 179-188.

4. H.L Stark and R.N. Ibrahim, *Estimating fracture toughness from small specimens*. Engineering Fracture Mechanics, 1986. **25**(4): p. 395-401.
5. Ibrahim., R.N. and J.W.H. Price, *CNT Small specimen Testing Procedure to Evaluate Fracture Toughness , operating Pressure equipment*. Institute of Metals and Materials of Australia 1997: p. 71-76.
6. R.N. Ibrahim , H.L.S., *Establishing K_{Ic} from eccentrically fatigue cracked small circumferentially grooved cylindrical specimens*. International Journal of Fracture, 1990. **44**: p. 179-188.
7. V. G. Laz'ko, V. E. Laz'ko , and B.M. Ovsyannikov, *Certain structural aspects of the fracture toughness of structural steel*. Strength of Materials. **13**(4): p. 527-532.
8. R. K Singh Raman, R.R., and R. N Ibrahim, *A novel approach to the determination of the threshold stress corrosion cracking (K_{ISCC}) using round tensile specimen*. Metallurgical and Materials Transaction A, 2006. **37A**: p. 2963-2973.
9. Rihan, R.O., *A Novel Fracture Mechanics Approach For The Determination of Susceptibility of Engineering Materials to Stress Corrosion Cracking*, in *Mechanical Engineering*. 2005, Monash Univeristy: Melbourne.
10. Ibrahim, R.N., *The Development of a small KIC specimen and its application to sustained load cracking in Aluminium Pressure vessels"*. 1989, University of New South Wales.
11. Sarvesh Pal, R.K. Singh Raman, and R.N. Ibrahim, *Determination of threshold stress intensity factor (K_{ISCC}) of simulated HAZ in caustic solution using circumferential notch tensile technique in Corrosion & Prevention 08*. 2008: Wellington NZ.
12. Arsenault, B. and E. Ghali, *Stress corrosion cracking of pressure vessel welded carbon steels*. International Journal of Pressure Vessels and Piping, 1991. **45**(1): p. 23-41.
13. Sarloglu, F., *The effect of tempering on susceptibility to stress corrosion cracking of AISI 4140 steel in 33% sodium hydroxide at 80°C*. Materials Science and Engineering A, 2001. **315**(1-2): p. 98-102.
14. Sangho Kim, Suk Young Kang, Sunghak Lee, Sei J. Oh, Soon- Ju kwon, Oo Hag Kim, and Jun Hwa Hong , *Correlation of the microstructure and fracture toughness of the heat-affected zones of an SA 508 steel* Metallurgical and Materials Transactions A, 2000. **31A**(4): p. 1107-1119.